CrossMark

ORIGINAL PAPER

Application of Convergence–Confinement Method in Analysis of Shallow Non-circular Tunnels

M. Mousivand · M. Maleki · M. Nekooei · M. R. Mansoori

Abstract Stress reduction factor, λ, is a dimensionless coefficient in two-dimensional (2D) analysis based on convergence confinement method (CCM) of tunnel which represents stress relaxation in the tunnel walls at different excavation steps. The aim of this paper is to look into the influencing factors on parameter λ around the tunnel walls using finite difference code in order to improve the accuracy of the CCM. For this purpose, four different ground types with various tunnel radii, depths and cross section shapes are considered. Finally, the 2D analysis using uniform and variable stress reduction factors determined in this paper is compared with the 3D analysis of the tunnel. The results of this study enhance our understanding of the role of geometrical and soil material parameters of tunnel on stress relaxation around tunnel walls. The tunnel depth, soil type and tunnel shape have great influence on λ. Variable stress reduction factor enables the convergence–confinement method to predict the realistic behavior of third dimension of the tunnel and can also be used as the best alternative to 3D models.

1 Introduction

Deformations and stresses analysis of tunnels is one of the main issues which has always been of interest for many researchers. Despite the fact that non-numerical methods, i.e. experimental, physical modeling and etc., are relatively good in predicting the ground–tunnel interaction behavior in some cases; in general, it is not possible to consider all the effects, parameters and boundary conditions that depend on the tunnel construction characteristics in these methods (Attewell 1977; Cairncross 1973; Chen et al. 2013; Mair et al. 1993; Meguid et al. 2008; O'ReiIIy and New 1982; Orr et al. 1976; Potts 1977; Schmidt 1974).

3D numerical analyses allow a designer to realistically model the tunneling process. These analyses can well model the ground behavior in front of a tunnel face and 3D arching phenomenon occurring around the tunnel face (Bloodworth 2002; Burd et al. 2000; Ng and Menzies 2004; Ng and Lee 2005). However, conducting such analyses is time-consuming and expensive. This means that 2D models are still more commonly used in initial estimates of tunnels than the 3D ones (Karakus 2007; Vlachopoulos and Diederichs 2014).

M. Mousivand · M. Nekooei · M. R. Mansoori
Department of Civil Engineering, Science and Research Branch, Islamic Azad University, Tehran, Iran

M. Maleki (✉)
Department of Civil Engineering, Bu-Ali Sina University, Hamadan, Iran
e-mail: Maleki@basu.ac.ir

Some assumptions are needed to simulate the third dimension of a tunnel in 2D models. There are several approaches for the 2D simulation of tunneling, such as the gap, convergence–confinement, volume loss control, gradual softening and disk calculation method (Lee and Rowe 1991; Panet and Guenot 1982; Potts and Zdravkovic 2001; Rowe et al. 1983; Schikora and Ostermeier 1988; Swoboda 1979; Swoboda et al. 1994).

Despite the developments made on the gap method by, Lee and Rowe (1991) it can be mainly used in shield circular tunnels and cannot be applicable for other excavation methods (Karakus 2007; Lee and Rowe 1991). The method of volume loss control, considering accurate estimation of volume loss, is an appropriate and useful approach. In addition, back analysis of tunnel can also be performed using this method (Potts and Zdravkovic 2001). The gradual softening and gap methods can be used to better understanding of multiple face tunneling. However, the tunnel excavation can be only performed with a reduction in the modulus of elasticity and effects of other ground parameters cannot be taken into consideration for excavation modeling (Schikora and Ostermeier 1988; Addenbrooke and Potts 2001; Atzl and Mayr 1994; Higgins et al.1996). The CCM can consider affecting the third dimension of the tunnel by three curves (ground reaction curve, longitudinal deformation profile and support characteristic curve) (Bouvard-Lecoanet 1988; Brown et al. 1983; Hoek and Brown 1980; Lombardi 1973; Panet 1995; Peila and Oreste 1995). In recent years, there has been an increasing amount of studies in improving the CCM (Bernaud and Rousset 1996; Corbetta 1991;

González-Nicieza et al. 2008; Graziani et al. 2005; Heidari and Tonon 2015; Oreste 2003; Sadeghiyan et al. 2016; Wong and Kaiser 1991).

CCM has a dimensionless coefficient λ, which represents stress relaxation in the tunnel walls at different excavation steps. This parameter is considered as a constant number in previous studies and effects of various factors such as ground materials, depth, radius and cross-section of tunnel are not taken into account. In addition, in most of the previous studies, this parameter has been determined based on no scientific reason and merely as a hypothetical choice; this is despite the fact that parameter λ has a direct effect on stresses and deformations around the tunnel.

This study aims to investigate the influencing factors including ground material set, radius, depth and cross section shape of tunnel and distance between face and lining of tunnel on stress reduction factor around the cross-section of a tunnel in soft ground using a series of parametric studies in order to improve the accuracy of the CCM in shallow tunnels. Finally, the 2D analysis, using unified and variable stress reduction factor obtained from the present study, was compared with the 3D analysis of the tunnel.

2 Convergence–Confinement Method (CCM)

The convergence–confinement method represents an efficient way for the analysis and design of tunnel lining. The stress reduction factor near the excavation face, as seen in Fig. 1, can be obtained by the following three curves:

Fig. 1 Basic parameters for determining stress reduction factor (λ) [based on Carranza-Torres and Fairhurst (2000), Fairhurst and Carranza-Torres (2002)]
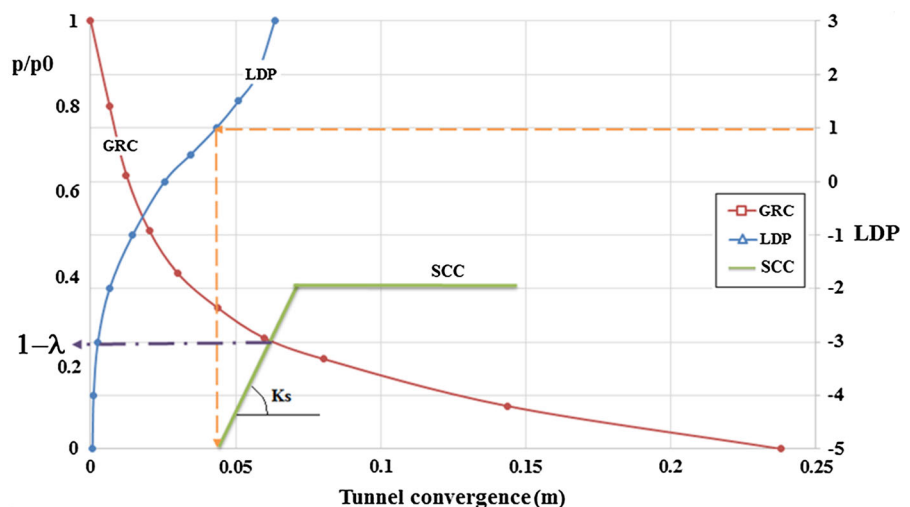
1. Ground reaction curve (GRC).
2. Longitudinal displacement profile (LDP).
3. Support characteristic curve (SCC).

To model the third dimension of tunnel in the 2D analysis using the convergence–confinement method, λ can be considered in three different modes (Fig. 2):

a. A section in front of the excavation face (Fig. 2a).
b. A section behind the tunnel face, between its face and lining (Fig. 2b).
c. A section far away from behind the tunnel face (Fig. 2c).

Different values for the stress reduction factor and stress in the tunnel walls for these three modes are presented in Fig. 2. Parameter σ_0 in this figure is the ground in situ stress.

In most previous researches, the GRC, SCC and LDP have been determined by analytical equations (González-Nicieza et al. 2008; Carranza-Torres and Fairhurst 2000; Lee et al. 1992). Analytical equations are generally used for the circular tunnel in isotropic conditions (Mitaim and Detournay 2005), while an alternative for estimating these curves is application of numerical analyses (Shin 2000).

2.1 Ground Reaction Curve (GRC)

This curve presents the convergence taking place around the tunnel at different pressures in the absence of lining. In order to determine exact curves, the numerical modeling of the tunnel was performed using
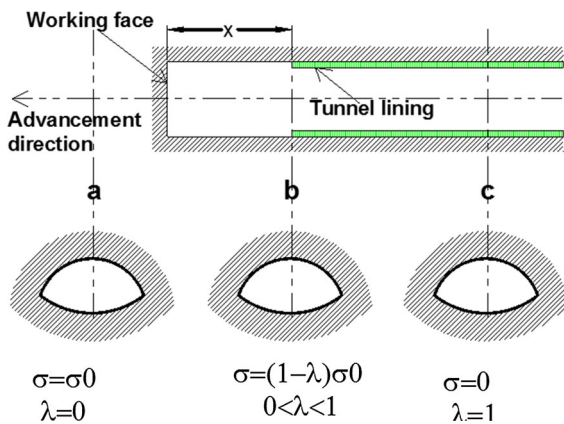

Fig. 2 Stress relaxation in the tunnel [based on González-Nicieza et al. (2008), Bernat and Cambou (1998)]

the finite difference code (FLAC 2D). GRC is obtained for all the points around the tunnel with the gradual reduction of confining pressure.

2.2 Support Characteristic Curve (SCC)

This curve represents the relationship between the inside pressure and deformation of tunnel walls. This curve can be calculated for different tunnel supports by considering the deformation occurring before the tunnel lining installation (Graziani et al. 2005; Oreste 2003): For a circular tunnel, elastic part of curve is obtained from Eq. (1);

$$P_S = K_S u_r \tag{1}$$

where K_s is the elastic hardening of the lining obtained from Eq. (2) and u_d is the start point of curve obtained by the LDP, based on the distance between the face and lining of tunnel (x).

$$k_s = \frac{E_{con}}{(1-\upsilon)} \frac{\left[r^2 - (r-t)^2 \right]}{\left[(1-2\upsilon)r^2 + (r-t)^2 \right]} \cdot \frac{1}{r} \tag{2}$$

The maximum allowable stress by the lining is determined by using Eq. (3);

$$p_{\max} = \frac{1}{2} \sigma_c \left[1 - \frac{(r-t)^2}{r^2} \right] \tag{3}$$

where r is the tunnel radius, t is the lining thickness, υ is the Poisson's ratio of the lining, E_c is the elastic modulus of concrete and σ_c is the concrete in 28 days' compressive strength.

In this paper, for any cross section curves (circular, horseshoe and double arch), precise SCC is obtained using finite difference code (FLAC 2D).

2.3 Longitudinal Deformation Profile (LDP)

This curve shows the displacement which occurs along the axis of the unlined tunnel. This curve is obtained through local instrumentation or a 3D simulation tool. In this paper, due to insufficient information from the longitudinal deformation of the tunnels in various ground and tunnel geometric conditions, a 3D analysis was performed using FLAC 3D software to determine the tunnel LDP.

3 Modeling and Parameters

3.1 Boundary Conditions

In numerical analyses, choosing geometric model parameters including location and type of lateral boundary and mesh size are directly affected on the accuracy of results. Basically, meshes must be fine enough in the region with stress concentration or near important details than the ones in other areas. During tunnel excavation, stress variations in this area are high. Thus, finer meshes must be used near the tunnel face to the extent possible. With increasing distance from the tunnel face, it is possible to reduce the density of mesh. In this study, a finite difference meshes, similar to the one in Fig. 3, was used to analyze the tunnel. Model dimensions were obtained by conducting a series of sensitivity analyses (Fig. 3).

Vertical boundaries should be so far away from the center of the tunnel so that ground displacement induced by tunneling is equal to zero. Such boundaries are modeled as horizontal rollers due to vertical displacements. Horizontal boundaries should be considered sufficiently below the tunnel where the impact of excavation on the boundaries can be neglected. In this case, by assuming the bedrock, the amount of displacement in the horizontal boundaries can be considered equal to zero.

3.2 Soil Model Parameters

In this study, the constitutive model of Mohr–Coulomb available in FLAC software is used. This model presents a linear elastic-perfectly plastic material behavior. Moreover, the model required five parameters for analysis (K: bulk modulus, G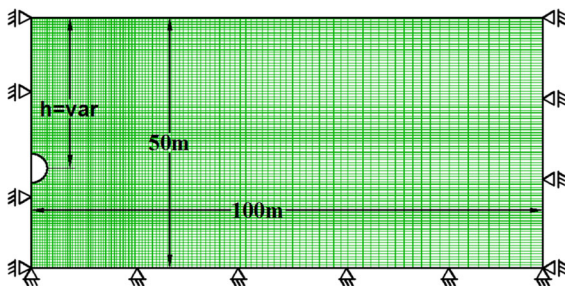: shear modulus, c: cohesion, φ: fiction angle and ψ: dilation angle) (Itasca 2002). In order to use all the aspects of research results, as shown in Table 1, four types of soils are used in this paper.

The required parameters of lining materials are presented in Table 2. The behavior of the tunnel lining is also considered as linear elastic-perfectly plastic.

4 Results and Discussion

In this study, three different tunnel cross-sections (circular, horseshoe and double arch) are utilized to measure the effects of the tunnel shape on the stress reduction factor in the CCM (Fig. 4). The shape of the upper part was similar for all the tunnels (semicircle with radius R). The shape of tunnels bottom part consists of the circle with radius R + 1 in the double arch, a rectangle with dimensions R × 2R in the horseshoe and a semicircle with radius R in the circle tunnel.

Table 1 Soil properties used for simulation of tunnel

	Unit	LS	DS	OC	NC
Density (ρ)	Kg/m^3	1800	2000	2100	1800
Shear modulus (G)	MPa	11.5	30.8	22.2	7.1
Bulk modulus (K)	MPa	25	66.7	66.7	33.3
Cohesion (C)	kPa	1	1	50	20
Friction angle (φ)	Degree	30	38	20	5

Table 2 Lining properties used in the analysis of tunnel

	Unit	
Elastic modulus (E)	GPa	26.5
Poisson's ratio (υ)		0.15
Thickness (t)	m	0.25

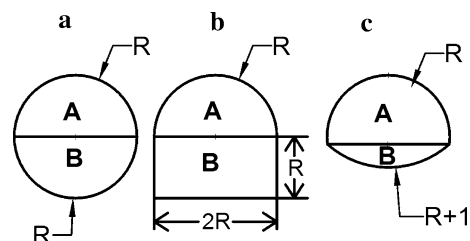**Fig. 3** Finite difference mesh for analyses (dimensions are in meter)

Fig. 4 Various cross-sections of the tunnel; **a** circular, **b** horseshoe, **c** double arch

4.1 Ground Reaction Curve

4.1.1 Effects of the Point Position on Tunnel Wall

In order to examine the effects of cross-section of tunnel on the GRC, depth, radius and type of soils were assumed constant. Three different locations around the tunnel (crown, wall and floor) were studied in this section. Figure 5 shows the tunnel convergence for various cross-sections. The horizontal axis of the charts is the total deformation (resultant of horizontal and vertical displacement) and the vertical axis is the ratio of confining stress (p) to in situ stress (p_0). As shown in Fig. 5, convergence taking place around the tunnel was different in various cross-sections. Accordingly, convergence in the horseshoe tunnel was the smallest amount and in the circular tunnel was the greatest. This demonstrated the differences in behavior of the three tunnel cross sections in the face of tunnel unloading. Another important point that could be obtained from Fig. 5 was the differences in the graphs of convergence at three points around the tunnel, which could reflect the different behaviors of various point positions of the tunnel regarding the tunneling. These results are consistent with those of other researchers such as González-Nicieza et al. (2008) and Amberg (2011).

4.1.2 Effects of Tunnel Depth

By assuming the soil type, radius and point position around the tunnel as constant, the convergence at different depths (10, 20, 30 and 40 m) is shown in Fig. 6. As can be seen in this figure, at a certain depth, the convergence was greater in the circular than that in the horseshoe cross-section. The convergence of the horseshoe was also more than that of the double arc cross section. However, the convergence was increased by increasing the tunnel depth. This demonstrated that the tunnel depth had significant effects on the GRC.

4.1.3 Effects of Tunnel Radius

By considering three different radii of 2, 3 and 4 m, the convergence of different cross-sections was investigated, the results of which are presented in Fig. 7. The curves were considered for over-consolidated clay at the depth of 10 m on the tunnel wall. In each tunnel
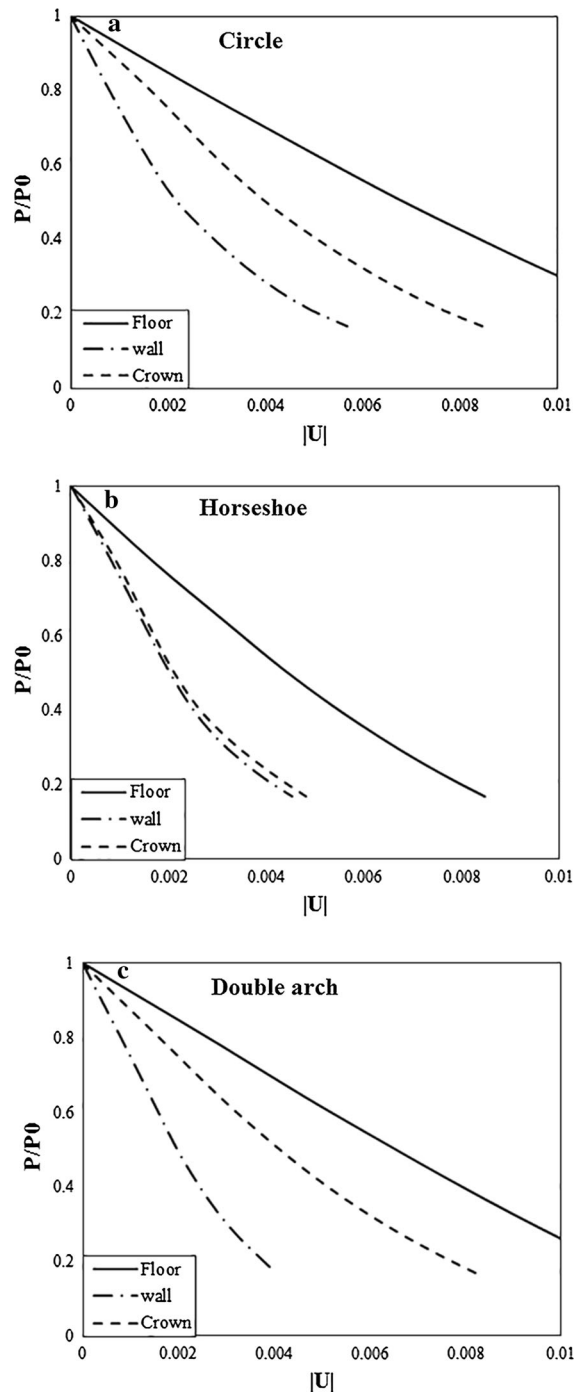

Fig. 5 Ground reaction curve in various point position around tunnel (radius 2 m, over-consolidated clay (OC), depth 10 m); **a** floor, **b** wall, **c** crown

cross-section, its convergence increased with increasing of tunnel radius. The GRC for the circular and horseshoe cross-sections were more similar than those
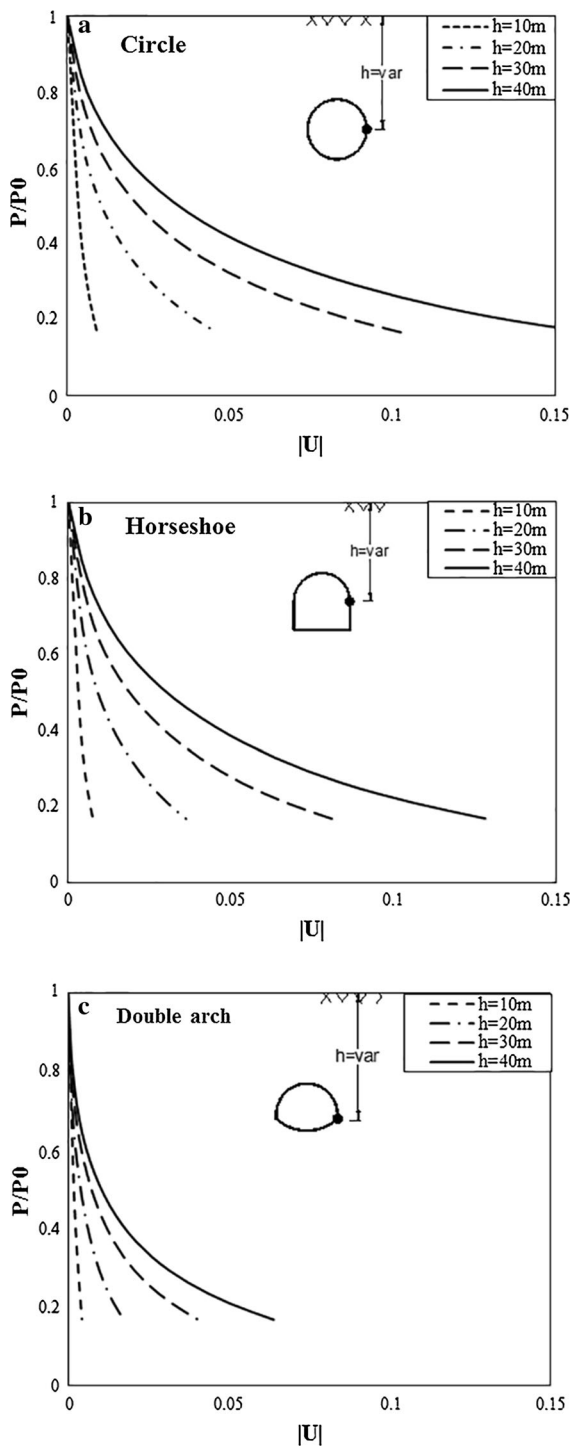
Fig. 6 Ground reaction curve of tunnel in various depth (radius 3 m, position: tunnel wall, over-consolidation clay); **a** Circle, **b** Horseshoe, **c** Double arch

for the double arch sections. By increasing the radius, the convergences in the circular and horseshoe cross-sections became closer.

4.1.4 Effects of Soil Type

By keeping the other variables constant, the ground convergence curves of different soil types for different cross-sections are presented in Fig. 8. As can be seen in the figure, the convergence occurring for each tunnel cross-section highly depended on the type of soils. In the clay material (Fig. 8b–d), the circular tunnel had greater convergence, while in the sand and gravel materials (Fig. 8a–c), the convergences of different cross-sections had fairly similar values.

4.2 Stress Reduction Factor (λ)

In this study, λ was determined at three surrounding points of the tunnel (crown, floor and wall) in each tunnel cross-section.

4.2.1 Effects of Point Position Around the Tunnel

Assuming the constant values of radius, depth, soil type and also the distance between the tunnel face and lining, the effect of point position around the tunnel was investigated for three different cross-sections, the results of which are presented in Fig. 9. In this figure, the vertical axis is the λ and the horizontal axis is different points around the tunnel (floor, wall and crown). The different behaviors of the λ could be seen in three various cross-sections which could be due to different tunnel shapes in lower parts. It demonstrated the importance of considering the effects of the point position around the tunnel to determine the stress reduction factor in different cross-sections.

By changing the horizontal angle from −90° (floor) to 90° (crown), stress reduction factor variations were about 5, 20 and 60% in double arch, horseshoe and circular cross section respectively. However, the change of horizontal angle from −90° (floor) to 0° (wall) caused the same variations of stress reduction factor (30%) in all different cross-sections.
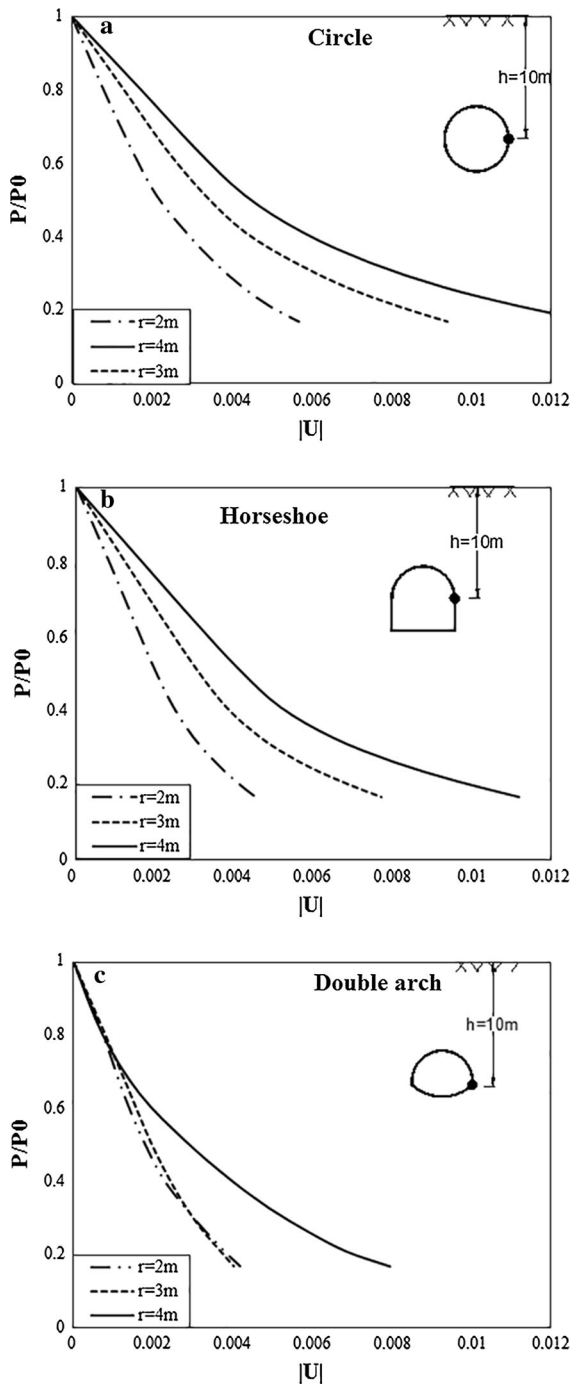
Fig. 7 Ground reaction curve of tunnel in various radius (depth 10 m, position: tunnel wall, soil type: over-consolidation clay); **a** r = 2 m, **b** r = 3 m, **c** r = 4 m
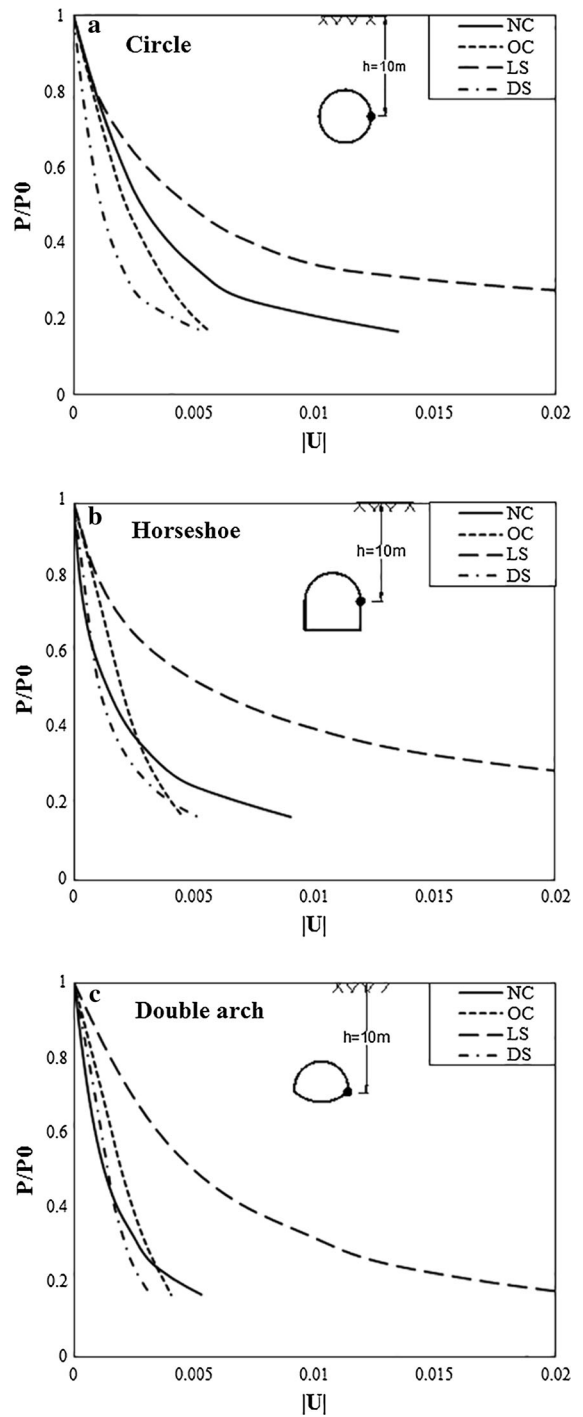

Fig. 8 Ground reaction curve in various soil types (radius: 2 m, depth: 10 m, position: tunnel wall); **a** Circle, **b** Horseshoe, **c** Double arch
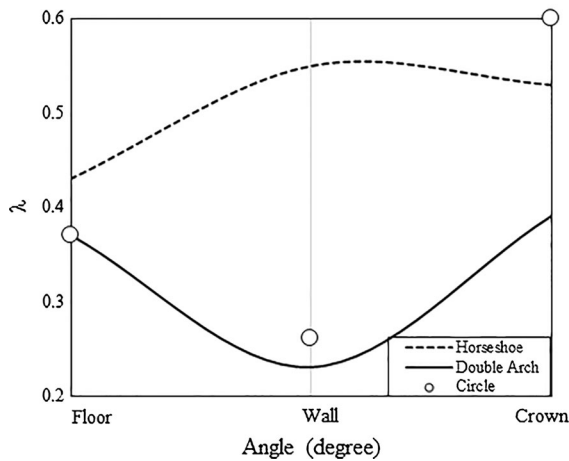
Fig. 9 Effect of point position on stress reduction factor (r = 2 m, depth = 10 m, over-consolidated clay (OC), x = 1 m)
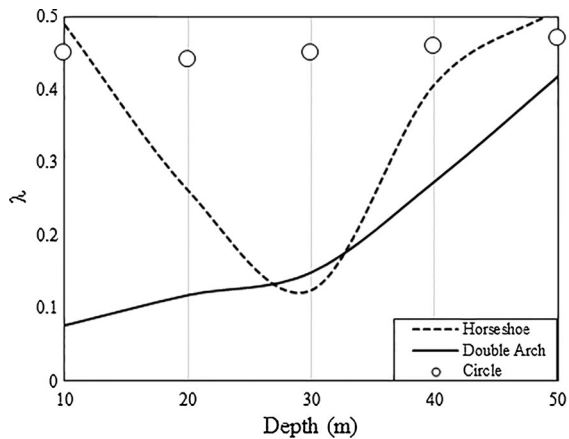

Fig. 10 Effect of depth on stress reduction factor (r = 2 m, point position: tunnel wall, over-consolidated clay, x = 1 m)

4.2.2 Effects of Tunnel Depth

In this section, by keeping all the other variables constant (soil type, radius, location on the cross section and distance between the tunnel face and lining), the effect of depth on the λ was studied in different cross-sections (Fig. 10). The results showed that the depth had a greater effect on the λ in the horseshoe than the other two cross-sections. In the horseshoe cross-section, the stress reduction factor decreased by about 70%, by increasing the depth from 10 to 30 m. However, by increasing the depth from 30 to 50 m, this parameter was increased about

300%. This trend was not observed in the other two tunnel shapes. In the circular tunnel, increase in tunnel depth from 10 to 50 m caused little variations (about 4%) in stress reduction factor. However, increasing depth from 10 to 50 m in the double arch tunnel caused stress reduction factor to be increased by about 400%.

4.2.3 Effects of Tunnel Radius

Radius also affected the stress reduction factor as shown in Fig. 11. The effect of radius was much greater in the horseshoe and double arch than in the circular tunnel. However, all the three cross sections had the same trend of λ in beyond 3 m radius of tunnel. The λ in various cross sections had approached almost the same value by increasing the tunnel radius. Increase of tunnel radius from 2 to 3 m caused the increase of stress reduction factor by about 5, 35 and 40% in circular, double arch and horseshoe cross sections respectively; however, by increasing the tunnel radius further (more than 3 m), stress reduction factor decreased by about 10, 20 and 15% respectively.

4.2.4 Effects of Soil Type

Soil type (loose or dense and cohesive or non-cohesive soil) had significant effects on the stress relaxation occurring around the tunnel. Such a finding was obtained by carrying out a series of analyses on four different soil types (normal consolidated clay (NC),
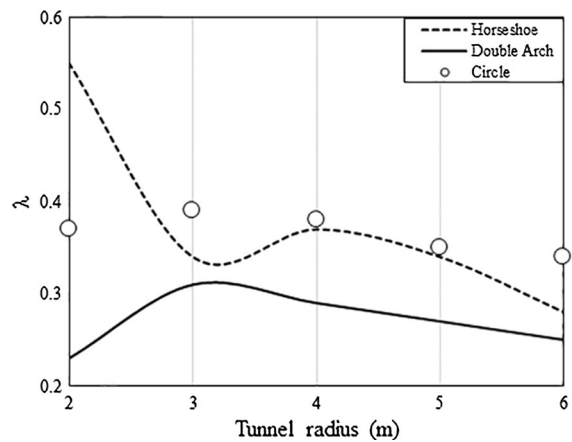

Fig. 11 Effect of tunnel radius on stress reduction factor (depth = 10 m, point position: tunnel wall, over-consolidated clay, x = 1 m)
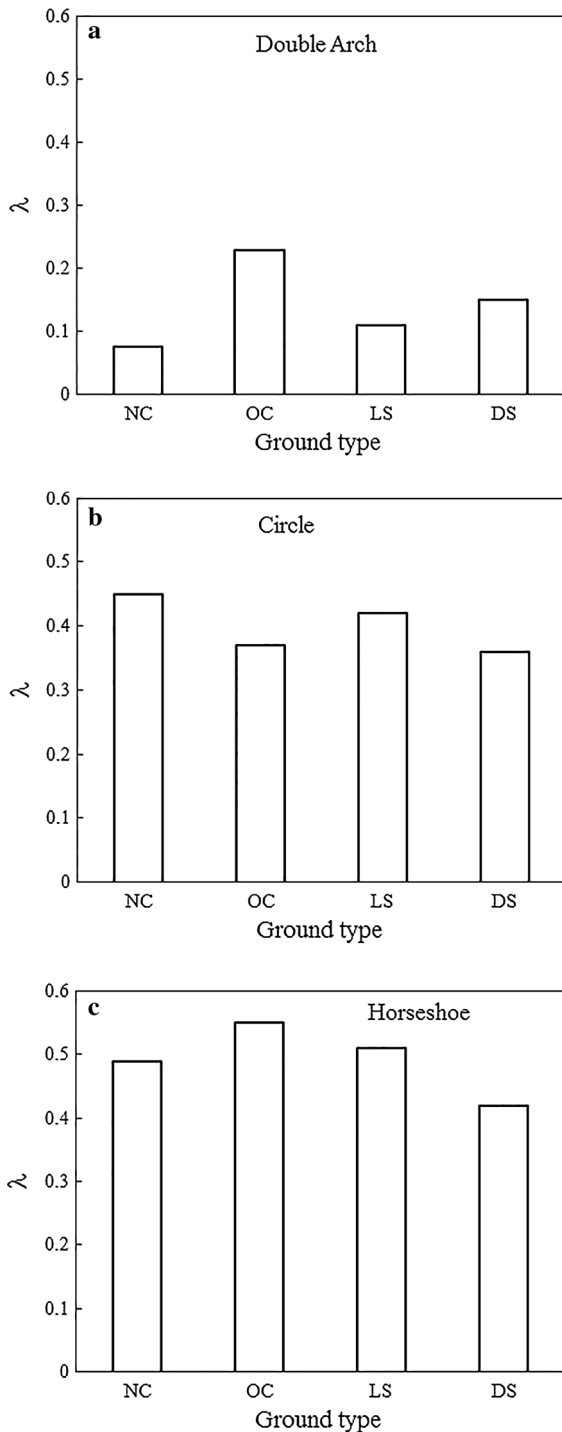
Fig. 12 Effect of soil type on stress reduction factor (r = 2 m, depth = 10 m, point position: tunnel wall, x = 1 m)

over consolidated clay (OC), dense sand and gravel (DS) and loose sand and gravel (LS)). The results are presented in Fig. 12. Similar to the variables

mentioned earlier, soil type behaved differently in various cross-sections. In granular soils (LS and DS), by increasing the soil strength, variations in λ for double arc, circular and horseshoe tunnel were about 27, 17 and 21% respectively. However, in cohesive soils (NC and OC), by increasing the soil strength, λ variations were 70, 20 and 12% respectively.

4.2.5 Effects of Distance Between the Tunnel Face and Lining

The effect of distance between the tunnel face and lining (x) on the stress reduction factor was also investigated in this study. The analyses results of the three cross-sections with the radius of 2 m at the depth of 10 m on the tunnel wall are shown in Fig. 13. By comparing the stress reduction factors in all the three cross-sections, a similar trend could be seen in all the cross-sections. Accordingly, by increasing distance from the tunnel face, the stress reduction factor was increased nonlinearly in all the three different cross-sections. However, stress reduction factor was different in each tunnel cross section. λ in circular and horseshoe cross-sections were more similar than those for the double arch section. By increasing the distance from tunnel face (more than 4 m), the stress reduction factor of circular and horseshoe cross-sections became close to the same value. By increasing the distance between face and lining of tunnel, stress reduction factor variations in circular, double arch and
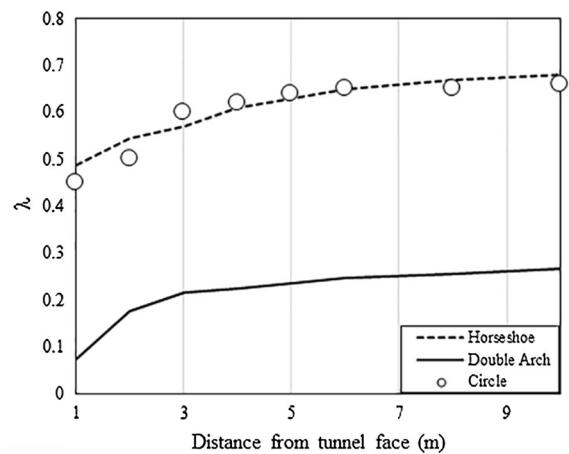

Fig. 13 Effect of distance from tunnel face on stress reduction factor (r = 2 m, depth = 10 m, point position: tunnel wall, over-consolidated clay)

Table 3 Cross section materials analyzed in the validation

| Parameters	Symbol	Unit	Tunnel cross section		
			Circle	Horseshoe	Double arch
Radius	r	m	2	3	4
Depth	h	m	40	20	10
Material set	–	–	LS	OC	CS
Distance between lining and tunnel face	x	m	1	2	1

horseshoe tunnel were 35, 200 and 35% respectively. As can be seen in Fig. 13, λ was independent of the distance from the tunnel face for more than 2R (R = tunnel radius). Therefore, the distance from tunnel face should be considered while determining the stress reduction factor in distances smaller than 2R.

4.3 Validation of Results

To validate the results of the present work, three different cross-sections were evaluated by 2D and 3D analyses, the details of which are presented in Table 3.

Stress reduction factor is variable at the points around the tunnel in the convergence–confinement method. However, for the purpose of simplification, constant values could be used for all the points around the cross-section, which is shown in Fig. 14.

λ_{uni} means that stress relaxation was equal at all the points around the tunnel and was obtained from the average of all stress reduction factors around the tunnel cross-section.
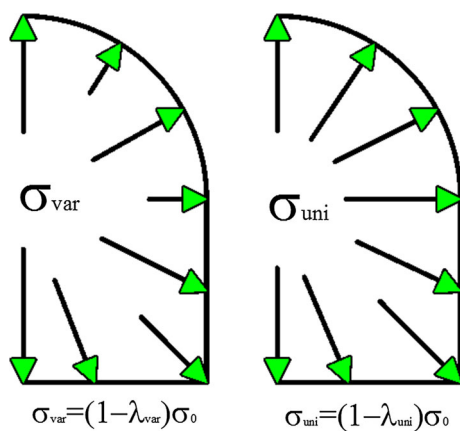

Fig. 14 Variable and uniform stress reduction factor used in the validation

λ_{var} means that stress relaxation had different values at all the points around the tunnel.

These values, using a FISH software program, were applied to the points around the tunnel, which led to a more realistic tunnel behavior in dealing with the unloading. The accuracy of the present method was investigated by comparing the horizontal and vertical displacements occurring around the tunnel in both 2D and 3D analyses.

4.3.1 Horizontal Displacements

The sections presented in Table 3 were assessed using 2D and 3D analyses. The results of the horizontal displacements of the ground at the distance of 6 m from the tunnel centerline are presented in Fig. 15a–c. In this section, the ground behavior could be clearly seen in response to tunneling. In these figures, the vertical and horizontal axes were depth and horizontal displacements respectively. Horizontal displacement curves were presented for three different cases (2D analysis with the same values of the stress relaxation, 2D analysis with the real values of the stress relaxation and 3D analysis). As shown in Fig. 15a–c, the horizontal displacements in the three cases were almost similar, which indicated that the 2D analysis could well simulate the third dimension of the tunnel. Therefore, the results obtained by taking parameter λ_{uni} in the analysis were fairly proper, which could be used in the tunnel initial estimation. However, the deformation obtained by the 2D analysis with uniform stress relaxation was different from that obtained by the 3D analysis. To increase the accuracy of the analysis and design of the tunnel, real stress relaxations should be used according to various points around the tunnel (λ_{var}), which was well converged with the 3D analysis results. This issue could be seen for the three sections located at different depths, soil types and distances from tunnel face.
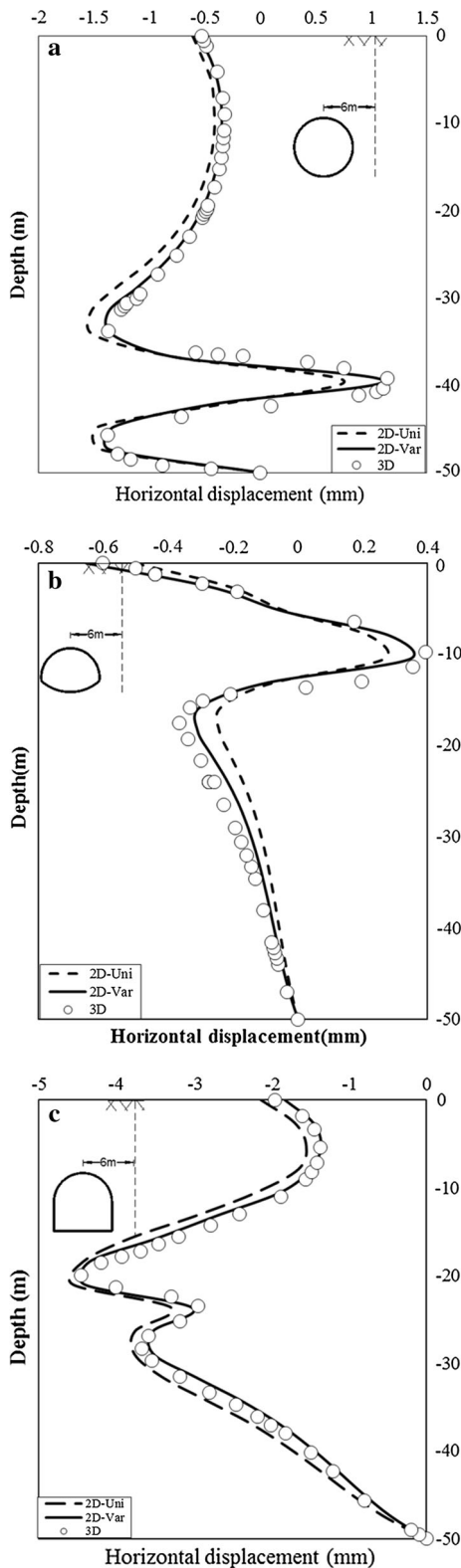
Fig. 15 Horizontal displacements at the distance of 6 m from tunnel centerline for various cross-sections; **a** circular, **b** horseshoe, **c** double arch tunnel

4.3.2 Vertical Ground Surface Movements

Vertical settlements occurring at the ground surface can also show the effects of stress relaxation on the 2D and 3D analyses. Figure 16 presents the ground surface settlements for three different cases (2D analysis with uniform and variable stress reduction
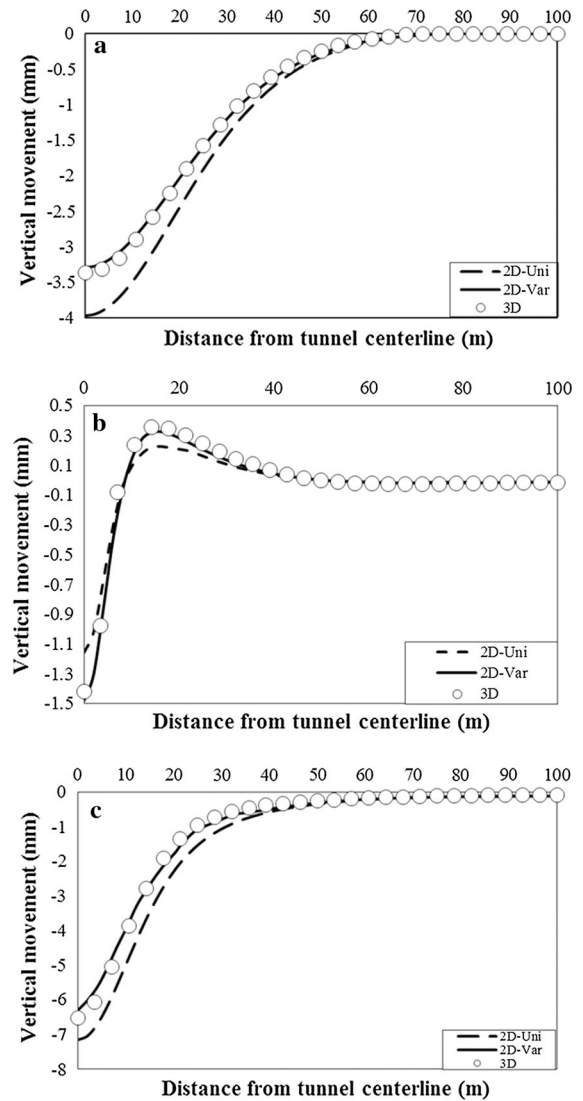

Fig. 16 Vertical movement of ground surface in various cross-sections; **a** circular, **b** horseshoe and **c** double arch tunnels

factor and 3D analysis). In these figures, the horizontal axis is the distance from the tunnel's centerline and the vertical axis is the ground movements induced by tunneling. By considering the stress reduction factor variable, the 2D ground settlements were more consistent with those of the 3D ones, as compared with the cases in which the stress reduction factor was considered constant. That was due to more realistic stresses and displacements induced by tunneling which could be modeled by considering the variable stress reduction factor. It represented a great number of errors in the analysis of tunnel considering uniform stress reduction factor.

5 Discussion

In this paper, the effect of third dimension of the tunnel with different cross sections (circular, horseshoe and double arch) was studied using 2D analysis based on CCM. For achieving this purpose, 2D analyses of shallow tunnels were carried out in three different sections. Firstly, ground reaction curves were investigated by considering the influence of different factors including point position around tunnel, depth, radius and cross-section of tunnel and soil type. The convergences were different in various point positions around tunnel walls in each cross section mentioned above. Depth and radius of tunnel, strength of granular soils and cohesion of cohesive soils had also substantial effects on tunnel convergences in each tunnel cross-section. However, tunnel convergence in different strength of granular soils had more similar trend than in various cohesion of cohesive soils.

In the next section, the affecting parameters on the stress reduction factor including point position, depth, radius and cross-section of tunnel and soil types were carried out using a series of numerical models. Stress reduction factor had different values all around tunnel walls in each cross section. The most variations of stress reduction factor occurred in crown to floor position. Increasing the tunnel radius from 2 to 3 m caused the increase of stress reduction factor in various cross sections by different trends. By increasing the radius more (from 3 to 6 m) or increasing the depth of tunnel, stress reduction factor was decreased. Soil types had also great effects on stress reduction factor. Increasing the strength parameters in granular soils (loose to dense soil) caused to variation stress

reduction factor by about 20% in all different cross sections. However, increasing the over consolidation ratio (OCR) of cohesive soils caused drastic variations in stress reduction factor in various tunnel cross sections. These variations had minimum values in horseshoe and circular tunnels and maximum value in double arch tunnel. Stress reduction factor had different values in different distances between face and lining of tunnel in all cross sections of tunnel.

Finally, the present study was verified by the 3D simulation of the tunnel in different cross-sections, depths, radii and soil types. Two different stress reduction factors (uniform and variable) were used in 2D analysis based on convergence–confinement method. Horizontal and vertical movements of ground in 2D analysis using both uniform and variable stress reduction factors by considering third dimension of the tunnel could be converged with the 3D analysis results. However, the variable stress reduction factor led to more reliable results of 2D analysis.

6 Conclusions

The major results obtained from the present study can be emphasized as follows:

1. The tunneling model using the 2D simulation based on CCM was able to simulate the realistic behavior of the third dimension of the tunnel through considering the variable stress reduction factor according to different points around the tunnel walls.
2. The 2D analysis process presented in this study was much faster than the 3D analysis with the same accuracy.
3. The stress reduction factor had different values for different depths which must be considered in the 2D analysis using CCM.
4. Due to the changes taking place in the tunnel face, the λ had different values in various tunnel radii. This was despite the fact that many researchers have considered the same values of λ for different tunnel radii.
5. The stress reduction factor was also dependent on the points around the tunnel. Moreover, any point around the tunnel took different values due to the different stresses and deformations caused by tunneling. Lack of attention to this issue can lead to large errors in the 2D analysis and design of the tunnel.

6. Comparing the 2D and 3D analyses showed that the results obtained by the 2D analyses using uniform stress reduction factors (average of stress reduction factors all around the tunnel) were relatively different from three dimensional analyses. However, this average can be used for initial estimates of tunnel.

7. Variable stress relaxation can accurately simulate the stress and deformation paths and can also be used as the best alternative for 3D analysis.

References

Addenbrooke T, Potts D (2001) Twin tunnel interaction: surface and subsurface effects. Int J Geomech 1(2):249–271

Amberg F (2011) For a correct interpretation of ground reaction curves. In: 12th ISRM Congress, International society for rock mechanics

Attewell P (1977) Ground movements caused by tunnelling in soil. In: Conference on Large Ground Movements and Structures, Cardiff, p 812–848

Atzl GV, Mayr JK (1994) FEM analysis of Heathrow NATM trial tunnel. In: Numerical methods in geotechnical engineering. Balkema, Rotterdam, pp 195–201

Bernat S, Cambou B (1998) Soil-structure interaction in shield tunnelling in soft soil. Comput Geotech 22(3):221–242

Bernaud D, Rousset G (1996) The 'new implicit method'for tunnel analysis. Int J Numer Anal Meth Geomech 20(9):673–690

Bloodworth A (2002) Three-dimensional analysis of tunneling effects on structures to develop design methods. Oxford University, UK

Bouvard-Lecoanet A, Colombet G, Esteulle F (1988) Ouvrages souterrains-Conception, réalisation, entretien, 2nd ed. Presses de L'Ecole Nationale des Ponts et Chaussées, Paris, p 286

Brown ET et al (1983) Ground response curves for rock tunnels. J Geotech Eng 109(1):15–39

Burd H et al (2000) Modelling tunnelling-induced settlement of masonry buildings. Proc Inst. Civ. Eng.Geotech Eng 143(1):17–30

Cairncross A (1973) Deformations around model tunnels in stiff clay in engineering department. Cambridge University, UK

Carranza-Torres C, Fairhurst C (2000) Application of the convergence–confinement method of tunnel design to rock masses that satisfy the Hoek-Brown failure criterion. Tunn Undergr Space Technol 15(2):187–213

Chen R-P et al (2013) Experimental study on face instability of shield tunnel in sand. Tunn Undergr Space Technol 33:12–21

Corbetta F Bernaud D, Nguyen Minh D (1991) Contribution à la méthode convergence-confinement par le principe de la similitude. Revue Française de Géotechnique 54, pp 5–12

Fairhurst C, Carranza-Torres C (2002) Closing the circle. In: Proceedings of the 50th annual geotechnical engineering conference

González-Nicieza C et al (2008) Influence of the depth and shape of a tunnel in the application of the convergence–confinement method. Tunn Undergr Space Technol 23(1):25–37

Graziani A, Boldini D, Ribacchi R (2005) Practical estimate of deformations and stress relief factors for deep tunnels supported by shotcrete. Rock Mech Rock Eng 38(5):345–372

Heidari M, Tonon F (2015) Ground reaction curve for tunnels with jet grouting umbrellas considering jet grouting hardening. Int J Rock Mech Min Sci 76:200–208

Higgins K et al. (1996) Numerical modelling of the influence of the Westminster Station excavation and tunnelling on the Big Ben clock tower. In: Proc. Int. Symp. on geotechnical aspects of underground construction in soft ground, pre-print vol., London

Hoek E, Brown ET (1980) Undeground excavations in rocks. Institution of Mining and metarllurgy, E & FN SPON

Itasca F (2002) Fast lagrangian analysis of continua, version 4.0 user's guide. Itasca Consulting Group. Inc., Thrasher Square East, Minneapolis, p 708

Karakus M (2007) Appraising the methods accounting for 3D tunnelling effects in 2D plane strain FE analysis. Tunn Undergr Space Technol 22(1):47–56

Lee K, Rowe R (1991) An analysis of three-dimensional ground movements: the Thunder Bay tunnel. Can Geotech J 28(1):25–41

Lee K, Rowe RK, Lo K (1992) Subsidence owing to tunnelling. I. Estimating the gap parameter. Can Geotech J 29(6):929–940

Lombardi G (1973) Dimensioning of tunnel linings with regard to constructional procedure. Tunnel and tunneling, No. 4, pp 340–351

Mair R, Taylor R, Bracegirdle A (1993) Subsurface settlement profiles above tunnels in clays. Geotechnique 43(2):315–320

Meguid M et al (2008) Physical modeling of tunnels in soft ground: a review. Tunn Undergr Space Technol 23(2):185–198

Mitaim S, Detournay E (2005) Determination of ground reaction curve for hyperbolic soil model using the hodograph method. Can Geotech J 42(3):964–968

Ng CW, Lee GT (2005) Three-dimensional ground settlements and stress-transfer mechanisms due to open-face tunnelling. Can Geotech J 42(4):1015–1029

Ng CWW, Simons CN, Menzies B (2004) A short course in soil-structure engineering of deep foundations, excavations and tunnels. Thomas Telford Services Limited, London

Oreste P (2003) Analysis of structural interaction in tunnels using the covergence–confinement approach. Tunn Undergr Space Technol 18(4):347–363

Orr T (1976) The behavior of lined and unlined model tunnel in stiff clay, in engineering. Cambridge University, UK

O'ReiIIy M, New B (1982) Settlements above tunnels in the UK—their magnitude and prediction. In: Proceedings of Tunnelling'82, London, p 173–181

Panet M, Guenot A (1982) Analysis of convergence behind the face of a tunnel: Tunnelling 82. In: proceedings of the 3rd international symposium, Brighton, 7–11 June, p 197–204. Publ London: IMM, . in International Journal of Rock

Mechanics and Mining Sciences and Geomechanics Abstracts. 1983. Pergamon

Panet M (1995) Le calcule des tunnels par la methode convergence-confinement. Presses ENPC, Paris

Peila D, Oreste P (1995) Axisymmetric analysis of ground reinforcing in tunnelling design. Comput Geotech 17(2):253–274

Potts D (1977) Behavior of lined and unlined tunnels in sand, in engineering department. Cambridge University, UK

Potts DM, Zdravkovic L (2001) Finite element analysis in geotechnical engineering: application, vol 2. Thomas Telford, London, p 427

Rowe R, Lo K, Kack G (1983) A method of estimating surface settlement above tunnels constructed in soft ground. Can Geotech J 20(1):11–22

Sadeghiyan R, Hashemi M, Moloudi E (2016) Determination of longitudinal convergence profile considering effect of soil strength parameters. Int J Rock Mech Min Sci 82:10–21

Schikora K, Ostermeier B (1988) Two-dimensional calculation model in tunneling-verification by measurement results and by spatial calculation. In: Sixth international conference on numerical methods in geomechanics, Innsbruck, Austria

Schmidt B (1974) Prediction of settlements due to tunneling in soil: three case histories. In: Proceedings of the second rapid excavation and tunneling conference, San Francisco, p 1179–1199

Shin J (2000) Numerical analysis of tunnelling in decomposed granite soil. Imperial College London (University of London), London

Swoboda G, Marence M, Mader I (1994) Finite element modelling of tunnel excavation. Int J Eng Model 6:51–63

Swoboda G (1979) Finite element analysis of the new austrian tunnelling method (NATM). In: Proceedings of the 3rd international conference on numerical methods in geomechanics, Aachen

Vlachopoulos N, Diederichs MS (2014) Appropriate uses and practical limitations of 2D numerical analysis of tunnels and tunnel support response. Geotech Geol Eng 32(2):469–488

Wong R, Kaiser P (1991) Performance assessment of tunnels in cohesionless soils. J Geotech Eng 117(12):1880–1901